

Evolution of InAs branches in InAs GaAs nanowire heterostructures

M. Paladugu, J. Zou, G. J. Auchterlonie, Y. N. Guo, Y. Kim, H. J. Joyce, Q. Gao, H. H. Tan, and C. Jagdish

Citation: [Applied Physics Letters](#) **91**, 133115 (2007); doi: 10.1063/1.2790486

View online: <http://dx.doi.org/10.1063/1.2790486>

View Table of Contents: <http://scitation.aip.org/content/aip/journal/apl/91/13?ver=pdfcov>

Published by the [AIP Publishing](#)

Articles you may be interested in

[The influence of the droplet composition on the vapor-liquid-solid growth of InAs nanowires on GaAs \(111\)B by metal-organic vapor phase epitaxy](#)

[J. Appl. Phys.](#) **104**, 114315 (2008); 10.1063/1.3033556

[Strain relaxation and stress-driven interdiffusion in InAs InGaAs InP nanowires](#)

[Appl. Phys. Lett.](#) **91**, 063122 (2007); 10.1063/1.2764446

[Structural characteristics of GaSb GaAs nanowire heterostructures grown by metal-organic chemical vapor deposition](#)

[Appl. Phys. Lett.](#) **89**, 231917 (2006); 10.1063/1.2402234

[Fabrication of InP InAs InP core-multishell heterostructure nanowires by selective area metalorganic vapor phase epitaxy](#)

[Appl. Phys. Lett.](#) **88**, 133105 (2006); 10.1063/1.2189203

[Defect-free InP nanowires grown in \[001\] direction on InP \(001\)](#)

[Appl. Phys. Lett.](#) **85**, 2077 (2004); 10.1063/1.1784548

An advertisement for the journal 'Computing: Science & Engineering'. It features a row of computer monitors in a library setting, each displaying the journal's cover. The cover art shows a colorful, abstract pattern resembling a galaxy or a complex data visualization. The text 'computing SCIENCE & ENGINEERING' is visible on the covers. At the bottom, the text reads 'AIP's JOURNAL OF COMPUTATIONAL TOOLS AND METHODS. AVAILABLE AT MOST LIBRARIES.' The 'computing SCIENCE & ENGINEERING' logo is also present in the bottom right corner of the advertisement.

Evolution of InAs branches in InAs/GaAs nanowire heterostructures

M. Paladugu

School of Engineering, The University of Queensland, Brisbane QLD 4072, Australia

J. Zou^{a),b)} and G. J. Auchterlonie

School of Engineering, The University of Queensland, Brisbane QLD 4072, Australia and Centre for Microscopy and Microanalysis, The University of Queensland, Brisbane QLD 4072, Australia

Y. N. Guo

School of Engineering, The University of Queensland, Brisbane QLD 4072, Australia

Y. Kim

Department of Physics, Dong-A University, Hadan-2-dong, Sahagu, Busan 604-714, Korea

H. J. Joyce, Q. Gao, H. H. Tan, and C. Jagadish^{a),c)}

Department of Electronic Materials Engineering, Research School of Physical Sciences and Engineering, The Australian National University, Canberra ACT 0200, Australia

(Received 17 August 2007; accepted 8 September 2007; published online 28 September 2007)

Branched nanowire heterostructures of InAs/GaAs were observed during Au-assisted growth of InAs on GaAs nanowires. The evolution of these branches has been determined through detailed electron microscopy characterization with the following sequence: (1) in the initial stage of InAs growth, the Au droplet is observed to slide down the side of the GaAs nanowire, (2) the downward movement of Au nanoparticle later terminates when the nanoparticle encounters InAs growing radially on the GaAs nanowire sidewalls, and (3) with further supply of In and As vapor reactants, the Au nanoparticles assist the formation of InAs branches with a well-defined orientation relationship with GaAs/InAs core/shell stems. We anticipate that these observations advance the understanding of the kink formation in axial nanowire heterostructures. © 2007 American Institute of Physics. [DOI: 10.1063/1.2790486]

Semiconductor nanowires (NWs) and their associated heterostructures exhibit novel and device applicable physical properties,¹⁻⁴ which has led to the fabrication of nanoelectronic and nano-optoelectronic devices, such as field-effect transistors,^{5,6} photodiodes,^{7,8} transistor arrays,⁹ and biosensors.¹⁰ The vapor-liquid-solid (VLS) mechanism, using metal nanoparticles (NPs) as nucleation sites, is a commonly used process for semiconductor NW growth, in which Au NPs have been generally used in this process.¹¹⁻¹³ This mechanism offers the flexibility to produce axial and radial NW heterostructures,^{12,13} which can be achieved by varying the vapor chemistry during NWs growth.¹³ Attainment of lateral lattice relaxation of misfit strain due to the smaller growth area is an inherent advantage of axial NW heterostructures, which enables the integration of high lattice mismatch materials with few or without misfit dislocations.¹² NWs of III-V semiconductors with multiple axial heterojunctions, such as GaP/GaAs^{13,14} and InP/InAs,^{15,16} have been studied in terms of their growth behavior and device applicability.

According to our recent study¹⁷ and Dick *et al.*,¹⁸ interfacial energy between the metal NPs and the semiconductor materials is the key parameter that determines the success of growing an axial NW heterostructure through the VLS mechanism. This has been clearly demonstrated in Au assisted initiation of GaAs/InAs and InAs/GaAs NW heterostructures, where the axial growth of GaAs on InAs NWs proceeds,¹⁹ but axial growth of InAs on GaAs NWs does not. In the latter case, the Au particle instead slides down the

original GaAs NW by preserving a Au-GaAs interface during InAs growth.¹⁷ This growth difference is attributed to a lower interfacial energy between Au and GaAs than between Au and InAs, and this phenomenon can have general applicability in NW heterostructures growth when the interfacial energies between NP and the NW composing materials are unequal.¹⁷ This downward movement of Au was also observed in InP and Ge growth on GaP NWs.¹⁸ The feasibility of multiple axial heterojunctions in the case of GaAs/GaP and InAs/InP NWs is most probably due to equal interfacial energies between NP and the NW composing materials.¹⁸ These phenomena may be further treated by the chemical tensions.²⁰

In this study, we demonstrate the role of Au NPs during the growth of InAs on GaAs NWs. The morphological and structural characteristics of resultant NW heterostructures were characterized by detailed electron microscopy. Based on these studies, the mechanism behind the morphological evolution of InAs/GaAs NW heterostructures has been determined.

InAs/GaAs NWs were grown using 30 nm diameter Au NPs in a horizontal flow low pressure (100 mbar) metal-organic chemical vapor deposition reactor at a growth temperature of 450 °C. As a first step, GaAs NWs were grown on a (111)B GaAs substrate for 30 min under trimethylgallium (TMG) and AsH₃ flow. Different InAs/GaAs NWs were produced by growing InAs NWs for 1, 3, 5, and 30 min on the GaAs NWs by switching off the TMG flow and switching on the trimethylindium (TMI) flow while maintaining constant AsH₃ flow. The flow rates of TMG, TMI, and AsH₃ were 1.2×10^{-5} , 1.2×10^{-5} and 5.4×10^{-4} mol/min, respectively. Scanning electron microscopy

^{a)} Authors to whom correspondence should be addressed.

^{b)} Electronic mail: j.zou@uq.edu.au

^{c)} Electronic mail: chennupati.jagadish@anu.edu.au

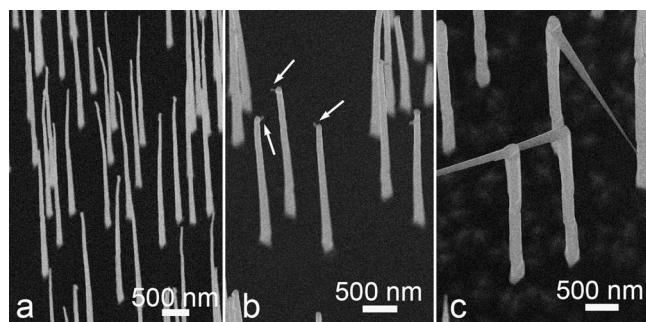


FIG. 1. SEM images of InAs/GaAs nanowires with different InAs growth times. (a), (b), and (c) correspond to 1, 5, and 30 min InAs growth, respectively. The images were taken when the substrate normal was tilted 20° away from the electron beam.

(SEM) (JEOL 890) and transmission electron microscopy (TEM) [JEOL2010, JEOL4010, FEI Tecnai F20 equipped with an energy dispersive spectrometry (EDS), and FEI Tecnai F30] investigations were carried out to understand the structural characteristics and chemical composition of the NWs. TEM specimens were prepared through ultrasonating the NWs in ethanol for 10 min and dispersing them on holey carbon films.

Figure 1 shows SEM images taken from InAs/GaAs NW heterostructures grown with different growth times for the InAs sections, and shows typical morphologies of the InAs/GaAs NW heterostructures. A small branch-like structure can be found near the tip of InAs/GaAs NWs with 5 min growth of InAs NW sections, as indicated by arrows in Fig. 1(b), but no such morphology is presented in NWs with 1 min growth of the InAs sections [see Fig. 1(a)]. In contrast, for the case of 30 min growth of InAs sections [Fig. 1(c)], the NWs have well-developed branches and the overall morphology of the NWs resembles stem-branch nanostructures. These SEM observations suggest that the branch growth initiated during first 5 min of InAs section growth, and it has progressed with further InAs growth.

To determine the mechanism behind this branched morphology in InAs/GaAs NW heterostructures, extensive TEM investigations were conducted on the NWs with different growth times of InAs sections. Figure 2(a) is a TEM image taken from a NW top portion with 1 min growth of the InAs section. As can be seen from Fig. 2(a), the Au NP has been displaced from the tip of the GaAs section onto the NW sidewall and, while maintaining an interface with the GaAs NW, has migrated down the GaAs NW sidewall during InAs growth.¹⁷ Figure 2(b) is a typical TEM image taken from an InAs/GaAs NW with 3 min growth of InAs section. The Moiré fringes and the strain contrast along the NW suggest that, with 3 min growth of InAs, radial growth of InAs has taken place around the GaAs NW sidewalls. It is of interest to note that the Au particles remain near the NW top regions, as shown in the inset of Fig. 2(b). Generally, in Au-assisted growth of NWs and their heterostructures, radial growth is a temperature dependent process.¹³ Similar to the cases of GaP/GaAs¹³ and GaAs/AlInP,²¹ we observed significant InAs radial growth (an InAs shell) on GaAs NWs at a growth temperature of 450°C . This observation indicates that, during the first 3 min growth of the InAs sections, radial growth of InAs becomes significant in comparison to the downward growth of InAs. Figure 2(c) is a typical TEM image taken from an InAs/GaAs NW with 5 min growth of the InAs section. In agreement with the SEM observations, a branch

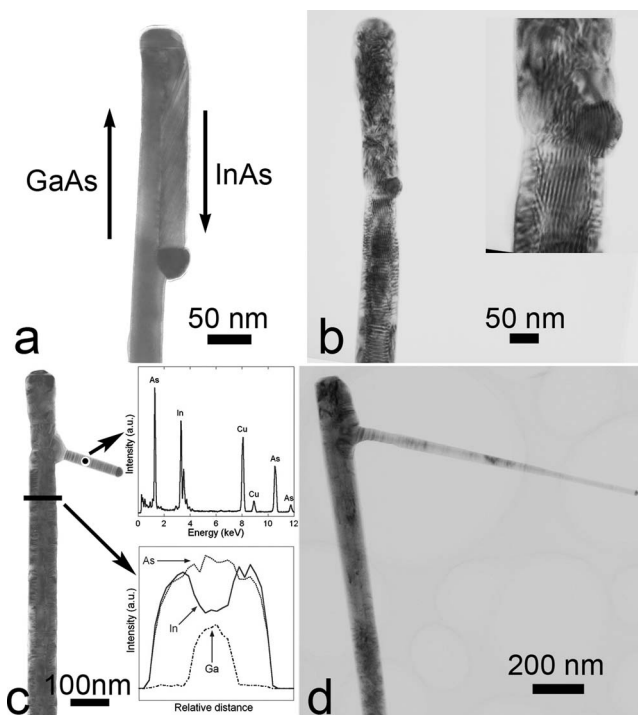


FIG. 2. TEM images of InAs/GaAs nanowires with different InAs growth times. (a), (b), (c), and (d) correspond to 1, 3, 5, and 30 min InAs growth, respectively. The inset in (b) is the magnified image of the nanowire portion at the Au nanoparticle. The insets in (c) show the results of the EDS analyses at different locations of the nanowire and the Cu peak is from the TEM grid.

has been developed from the NW with Au NP at the tip of the branch. The EDS analysis conducted on the NW heterostructures shows that the branch is composed of InAs and the stem has a core-shell structure of GaAs and InAs, as shown in the insets of Fig. 2(c). These results suggest that radial InAs growth prevents further downward movement of the Au NP. Once the Au NPs' downward movement ceases, the growth direction changes and the Au assisted growth of InAs branches initiates under further supply of In and As vapor reactants.

Under the conditions of thermodynamic equilibrium, the Au NP will maintain an interface with GaAs which directs the downward movement of the Au NP during the initial stage of InAs growth.¹⁷ However, these experimental results indicate that, with continuing supply of In and As vapor reactants, the Au NP-GaAs sidewall interface can no longer be maintained due to the formation of the InAs shell surrounding the GaAs sidewalls. As a result, axial growth of InAs NW branches initiates under further supply of In and As vapor reactants, via the VLS mechanism.¹⁷ Figure 2(d) shows an InAs/GaAs NW with a 30 min growth of the InAs section, in which a well developed InAs NW branch with respect to its stem can be clearly seen. Careful analysis of this branched NW shows that significant radial growth of InAs around the main stem has taken place, as evidenced by the increased stem diameter when compared with the NW shown in Fig. 2(c).

To understand the structural characteristics of the stem-branch morphology of the grown NWs, detailed TEM investigations were performed. Figure 3(a) is a TEM image of a typical NW and shows the stem-branch junction. Figures 3(b)–3(d) are selected area electron diffraction patterns taken, respectively, from the stem region, the branch region,

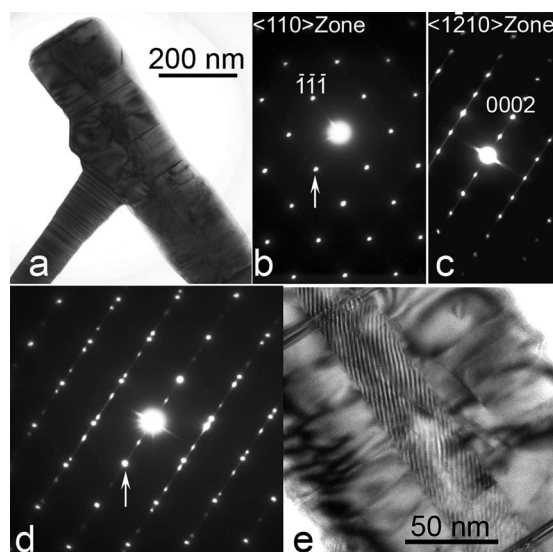


FIG. 3. (a) TEM image showing a junction of stem and branch. (b), (c), and (d) are the selected area diffraction patterns taken on the stem, branch, and their junction region, respectively. (e) High magnification TEM image of stem portion showing Moiré fringes in the core and strain contrast in the shell.

and their junction region, where the orientation between the NW and the electron beam remains unchanged. Figure 3(b) shows a $\langle 110 \rangle$ zone-axis diffraction pattern of the zinc-blende structure, while Fig. 3(c) shows a $\langle 1\bar{2}10 \rangle$ zone-axis diffraction pattern of the wurtzite structure, indicating that the stem has the zinc-blende structure and the branch has the wurtzite structure. Figure 3(d) shows two overlapped diffraction patterns originated from the branch and the stem, respectively, where the $\pm 0002^*$ reflections corresponding to the branch and a pair of $\{111\}^*$ reflections corresponding to the stem are overlapped. Since the NWs grew vertically on the $\{111\}B$ GaAs surface, we can define the growth direction of NW stems as parallel to the $[\bar{1}\bar{1}\bar{1}]$ direction. Based on this index, other three equivalent $\langle 111 \rangle B$ directions will be $[\bar{1}11]$, $[1\bar{1}1]$, and $[11\bar{1}]$, which have an angle of 109.5° with the $[\bar{1}\bar{1}\bar{1}]$ direction.²² We deduce that the atomic planes corresponding to the diffraction spot marked by an arrow [Figs. 3(b) and 3(d)] must belong to $\langle 111 \rangle B$ of the stem, and this diffraction spot overlaps with one of the $\pm 0002^*$ reflections that is parallel to the branch growth direction [Fig. 3(d)]. From crystallography, the $\langle 111 \rangle B$ direction in the zinc-blende structure is equivalent to the $[000\bar{1}]$ direction in the wurtzite structure. Therefore, we anticipate that the growth direction of the branch is along the $[000\bar{1}]$ direction and it grows epitaxially on the stem, i.e. along one of the $\langle 111 \rangle B$ directions of the stem (other than the stem's growth direction). Generally in VLS growth, $\langle 111 \rangle B$ is commonly observed growth direction of III-V semiconductor NWs, which might be attributed to the lower interfacial energy of $(111)B$ surfaces with liquid Au NPs.

It should be noted that there is only one set of diffraction pattern in Fig. 3(b) although the stem has the GaAs/InAs core/shell structure [see Fig. 2(c)]. Furthermore, the overlap of a pair of 111^* reflections from the stem with $\pm 0002^*$ reflections from the branch indicates that the diffraction pattern shown in Fig. 3(b) should have a lattice parameter of InAs.

To clarify this point, we have taken a high magnification bright-field image from the stem region and the result is presented in Fig. 3(e). The existence of the GaAs core is evidenced by the Moiré fringes in the middle region of the NW, and this core is significantly thinner than the InAs shell, which might cause the main contribution of InAs to the electron diffraction pattern [Fig. 3(b)]. Such a thick shell must have formed due to the 30 min growth of InAs, as radial InAs growth continued simultaneously with the InAs branch growth.

In conclusion, we have demonstrated the evolution of InAs branches during InAs growth on GaAs NWs by growing the InAs sections for different durations and by detailed SEM and TEM investigations. The evolution can be summarized as follows: (i) the downward movement of the Au NP is terminated by the radial growth of InAs around the sidewalls of a GaAs NW; (ii) with further InAs growth, InAs axial growth initiates from that Au NP and progresses along a $\langle 111 \rangle B$ direction which is inclined to the GaAs/InAs core-shell stem. As a consequence, branched InAs NWs are formed.

The Australian Research Council is acknowledged for the financial support of this project. One of the authors (M.P.) acknowledges the support of an International Postgraduate Research Scholarship.

- ¹Y. Huang, X. F. Duan, and C. M. Lieber, *Small* **1**, 142 (2005).
- ²C. Thelander, P. Agarwal, S. Brongersma, J. Eymery, L. F. Feiner, A. Forchel, M. Scheffler, W. Riess, B. J. Ohlsson, U. Gosele, and L. Samuelson, *Mater. Today* **9**, 28 (2006).
- ³P. J. Pauzauskis and P. Yang, *Mater. Today* **9**, 36 (2006).
- ⁴H. J. Fan, P. Werner, and M. Zacharias, *Small* **2**, 700 (2006).
- ⁵O. Hayden, M. T. Bjork, H. Schmid, H. Riel, U. Drechsler, S. F. Karg, E. Lortscher, and W. Riess, *Small* **3**, 230 (2007).
- ⁶S. A. Dayeh, D. P. R. Aplin, X. T. Zhou, P. K. L. Yu, E. T. Yu, and D. L. Wang, *Small* **3**, 326 (2007).
- ⁷R. Agarwal and C. M. Lieber, *Appl. Phys. A: Mater. Sci. Process.* **85**, 209 (2006).
- ⁸O. Hayden, R. Agarwal, and C. M. Lieber, *Nat. Mater.* **5**, 352 (2006).
- ⁹F. Patolsky, B. P. Timko, G. H. Yu, Y. Fang, A. B. Greytak, G. F. Zheng, and C. M. Lieber, *Science* **313**, 1100 (2006).
- ¹⁰F. Patolsky, G. F. Zheng, and C. M. Lieber, *Anal. Chem.* **78**, 4260 (2006).
- ¹¹J. Zou, M. Paladugu, H. Wang, G. J. Auchterlonie, Y. N. Guo, Y. Kim, Q. Gao, H. J. Joyce, H. H. Tan, and C. Jagadish, *Small* **3**, 389 (2007).
- ¹²Y. N. Guo, J. Zou, M. Paladugu, H. Wang, Q. Gao, H. H. Tan, and C. Jagadish, *Appl. Phys. Lett.* **89**, 231917 (2006).
- ¹³M. A. Verheijen, G. Immink, T. de Smet, M. T. Borgstrom, and E. Bakkers, *J. Am. Chem. Soc.* **128**, 1353 (2006).
- ¹⁴M. T. Borgstrom, M. A. Verheijen, G. Immink, T. de Smet, and E. Bakkers, *Nanotechnology* **17**, 4010 (2006).
- ¹⁵M. T. Bjork, B. J. Ohlsson, T. Sass, A. I. Persson, C. Thelander, M. H. Magnusson, K. Deppert, L. R. Wallenberg, and L. Samuelson, *Appl. Phys. Lett.* **80**, 1058 (2002).
- ¹⁶M. T. Bjork, C. Thelander, A. E. Hansen, L. E. Jensen, M. W. Larsson, L. R. Wallenberg, and L. Samuelson, *Nano Lett.* **4**, 1621 (2004).
- ¹⁷M. Paladugu, J. Zou, Y. N. Guo, G. J. Auchterlonie, Q. Gao, H. J. Joyce, H. H. Tan, C. Jagadish, and Y. Kim, "Novel Growth Phenomena Observed in Axial InAs/GaAs Nanowire Heterostructures," *Small* (to be published).
- ¹⁸K. A. Dick, S. Kodambaka, M. C. Reuter, K. Deppert, L. Samuelson, W. Seifert, L. R. Wallenberg, and F. M. Ross, *Nano Lett.* **7**, 1817 (2007).
- ¹⁹B. J. Ohlsson, M. T. Bjork, A. I. Persson, C. Thelander, L. R. Wallenberg, M. H. Magnusson, K. Deppert, and L. Samuelson, *Physica E (Amsterdam)* **13**, 1126 (2002).
- ²⁰N. Li, T. Y. Tan, and U. Gosele, *Appl. Phys. A: Mater. Sci. Process.* **86**, 433 (2007).
- ²¹N. Skold, J. B. Wagner, G. Karlsson, T. Hernan, W. Seifert, M. E. Pistol, and L. Samuelson, *Nano Lett.* **6**, 2743 (2006).
- ²²D. B. Holt, *J. Mater. Sci.* **23**, 1131 (1988).